HTML ABSTRACT + LINKS

JOURNAL OF APPLIED PHYSICS **97**, 063503 (2005)

Analysis of copper-rich precipitates in silicon: Chemical state, gettering, and impact on multicrystalline silicon solar cell material

Tonio Buonassisi[a)]
Applied Science and Technology Group, University of California, Berkeley, California 94720 and Lawrence Berkeley National Laboratory, Berkeley, California 94720

Matthew A. Marcus
Advanced Light Source, Lawrence Berkeley National Laboratory, Berkeley, California 94720

Andrei A. Istratov[b)]
Electronics Research Laboratory, University of California, Berkeley, California 94720 and Lawrence Berkeley National Laboratory, Berkeley, California 94720

Matthias Heuer
Lawrence Berkeley National Laboratory, Berkeley, California 94720 and University of Leipzig, Scharnhorststrasse 20, D-04275 Leipzig, Germany

Theodore F. Ciszek
Siliconsultant, P.O. Box 1453, Evergreen, Colorado 80437

Barry Lai and Zhonghou Cai
Advanced Photon Source, Argonne National Laboratory, Argonne, Illinois 60439

Eicke R. Weber
Department of Materials Science and Engineering, University of California, Berkeley, California 94720 and Lawrence Berkeley National Laboratory, Berkeley, California 94720

(Received 23 September 2004; accepted 13 October 2004; published online 1 March 2005)

In this study, synchrotron-based x-ray absorption microspectroscopy (μ-XAS) is applied to identify the chemical states of copper-rich clusters within a variety of silicon materials, including as-grown cast multicrystalline silicon solar cell material with high oxygen concentration and other silicon materials with varying degrees of oxygen concentration and copper contamination pathways. In all samples, copper silicide (Cu_3Si) is the only phase of copper identified. It is noted from thermodynamic considerations that unlike certain metal species, copper tends to form a silicide and not an oxidized compound because of the strong silicon–oxygen bonding energy; consequently the likelihood of encountering an oxidized copper particle in silicon is small, in agreement with experimental data. In light of these results, the effectiveness of aluminum gettering for the removal of copper from bulk silicon is quantified via x-ray fluorescence microscopy, and a segregation coefficient is determined from experimental data to be at least $(1-2)\times 10^3$. Additionally, μ-XAS data directly demonstrate that the segregation mechanism of Cu in Al is the higher solubility of Cu in the liquid phase. In light of these results, possible limitations for the complete removal of Cu from bulk mc-Si are discussed. © *2005 American Institute of Physics*. [DOI: 10.1063/1.1827913]

I. INTRODUCTION

Copper is an ubiquitous contaminant in silicon-based device technology that can be easily introduced into the bulk of silicon wafers. According to the existing data on solubility and diffusivity of Cu in Si,[1–3] at only 425 °C the equilibrium solubility of Cu in Si is as high as 10^{13} cm^{-3}, and the diffusivity is such that Cu can traverse 220 μm of single-crystalline p-type silicon in under 10 s ($\lambda=\sqrt{4Dt}$). According to the current understanding of the electrical properties and defect interactions of copper in silicon,[4,5] interstitial copper is a shallow donor with relatively benign electrical activity. On the other hand, copper-rich precipitates are known to severely reduce the minority-carrier diffusion length by forming bands of states within the silicon band gap, thereby providing very effective pathways for recombination.[6–10]

The precipitation of copper is unfavorable in structurally perfect p-type silicon because of the significant lattice strains involved in the formation of copper-rich precipitates,[11] possibly limited by the relatively lower diffusivity of ejected silicon self-interstitials, compounded with the energy required to change the charge state of Cu upon precipitation.[5] Copper precipitation in bulk p-type silicon can occur if the Cu contamination level is high and the chemical driving force for precipitation is sufficient to overcome the barrier for precipitation.[8,9,12–14] More importantly, even in low concentrations copper readily precipitates in the presence of heterogeneous nucleation sites, such as stacking faults or certain types of dislocations.[15–18] It is also known that metal-rich clusters can be incorporated into structural defects during crystal growth.[19]

[a)]Author to whom correspondence should be addressed; electronic mail: buonassisi@alumni.nd.edu
[b)]Electronic mail: istratov@socrates.berkeley.edu

 © 2005 American Institute of Physics

Downloaded 20 Apr 2005 to 131.243.76.24. Redistribution subject to AIP license or copyright, see http://jap.aip.org/jap/copyright.jsp

Multicrystalline silicon (mc-Si), the cost-effective material out of which an increasing 50% of solar cell modules are currently produced,[20] typically contains high transition-metal concentrations combined with a high density and variety of structural defects. Not surprisingly, copper-rich particles have been observed at structural defects in poorly performing regions of mc-Si solar cell material,[21–25] complementing neutron activation analysis data reporting Cu concentrations in mc-Si as high as 10^{13} cm^{-3}.[26] While Cu-rich clusters are undoubtedly not the only type of defect responsible for reducing the efficiencies of mc-Si solar cells, their known recombination activity and repeated observation in poorly performing regions indicate that they most certainly can be a contributing factor.

The chemical states of these Cu-rich clusters have wide-reaching implications for predicting the stability of these clusters, and ultimately, their impact upon mc-Si solar cell devices.[22,27] For example, it is much more difficult to dissolve and getter copper from copper oxide or copper silicate clusters than from copper silicide, due to the higher binding energy of the metal atoms to those compounds.[27] Previous studies that have attempted to determine the chemical state of Cu-rich clusters in Si are largely restricted to transmission electron microscopy (TEM)-based energy dispersive x-ray spectroscopy and diffraction analyses of copper precipitates in samples prepared by in-diffusion of unusually high Cu concentrations, or grown from a heavily Cu-contaminated melt.[28–33] In these studies, a species of copper silicide, η-Cu_3Si, is the predominantly observed phase.

The question arises as to whether copper-rich clusters in intentionally contaminated samples are of a phase identical to that found in samples containing lower Cu concentrations, representative of what one might encounter in mc-Si without intentional contamination. Studies of these lower Cu concentrations are now possible with synchrotron-based x-ray microprobe techniques, due to the higher sensitivities and large scanning volumes of these techniques.[21,22] A recent synchrotron-based x-ray absorption spectroscopy (μ-XAS) study found that gettering-resistant Cu-rich clusters in oxygen-rich silicon had a shift in the Cu absorption edge to higher energies, interpreted as a possible indication that oxidized Cu-rich clusters may have formed.[27]

The objective of this study is to clarify these discrepancies in the literature, and to determine the chemical states of copper-rich particles located in a variety of silicon-based materials with varying degrees of oxygen concentration and Cu contamination pathways: float-zone silicon (FZ-Si) with copper introduced into the melt during crystal growth, copper-diffused $Si_{0.98}Ge_{0.02}/Si$ misfit dislocations, copper-diffused Czochralski silicon (CZ-Si) with oxygen precipitates, and as-grown mc-Si without any intentional Cu contamination. A discussion of the most probable oxidation states of copper-rich and other metal-rich clusters in silicon ensues.

Following the experimental identification and discussion of the chemical state of Cu-rich clusters in Si, it is of interest to quantify the effectiveness of the removal of Cu from bulk Si by aluminum gettering. Since Al is used as the ohmic back surface contact material for most silicon-based solar cells, aluminum gettering is a standard part of silicon solar cell processing. It has been reported that copper is readily gettered from silicon to aluminum even during a medium-temperature anneal,[34–37] yet that some Cu may resist gettering.[27] Herein, we report the chemical state and distribution of Cu within an Al gettering layer of variable thickness, estimate a segregation coefficient based on x-ray fluorescence microscopy (μ-XRF) data, and discuss the possible physical mechanisms that oppose the complete gettering of Cu in mc-Si to the Al gettering layer.

II. METHODOLOGY

Copper-rich clusters in four types of silicon materials, with varying amounts of oxygen and intentional copper contamination, were investigated in this study. Sample specifications are as follows:

Sample 1: Float-zone silicon intentionally contaminated with $3-4\times10^{16}$ Cu cm^{-3} during crystal growth. Float-zone crystals were grown at the National Renewable Energy Laboratory (see Ref. 38 for details). The particular crystal-growth conditions lead to a high density of structural defects. With no intentional *n*- or *p*-type doping, the actual conductivity of the sample was *n*-type, as evidenced by the rectifying behavior of a thin Pd diode evaporated on the polished and chemically cleaned surface.

Sample 2: Misfit dislocation heterostructure, consisting of a 2-μm-thick *n*-type $Si_{0.98}Ge_{0.02}$ middle layer between a 2.5-μm *n*-type silicon bottom buffer layer on a (001) silicon substrate and a 2.5-μm-thick *n*-type silicon cap layer. At the two interfaces between the SiGe and Si layers, a network of 60° misfit dislocations forms parallel to the surface and propagates in the $\langle 110 \rangle$ directions, intersecting at 90° angles. Copper was intentionally diffused at 800 °C. Samples were fabricated at North Carolina State University (U.S.A.) and copper-contaminated at King's College (U.K.); further details of sample preparation can be found in Ref. 39.

Sample 3: Czochralski silicon containing approximately 1.8×10^{6} cm^{-3} oxygen precipitates and approximately 1.5 $\times10^{15}$ cm^{-3} boron was chosen because of the high density of precipitation sites for metals and high precipitated oxygen concentration. The sample was intentionally contaminated with Cu and annealed at 1200 °C in a forming gas (N_2 $+5\%\,H_2$) ambient for 30 min. The anneal was terminated by an air cool.

Sample 4: As-grown, cast mc-Si wafer extracted from near the bottom of the cast mc-Si ingot, where the interstitial oxygen concentration can be as high as 10^{18} cm^{-3}.

To determine the precise location of copper nano- and microclusters inside each sample, synchrotron-based x-ray fluorescence microscopy (μ-XRF) was performed at Beamlines 10.3.1 and 10.3.2 of the Advanced Light Source (ALS) at Lawrence Berkeley National Laboratory, and at Beamline 2-ID-D of the Advanced Photon Source (APS) of Argonne National Laboratory. At the time of measurement, the focusing optics of ALS Beamlines 10.3.1 and 10.3.2, respectively, were adjusted to achieve optimum spot sizes (spatial resolutions) of 2×3 μm^2 and 5×7 μm^2, at fluxes of ~1 $\times10^9$ photons/s. The zone plate optics of APS Beamline 2-ID-D achieved a spot size of 200 nm in diameter, with a

Downloaded 20 Apr 2005 to 131.243.76.24. Redistribution subject to AIP license or copyright, see http://jap.aip.org/jap/copyright.jsp

flux $\sim 10^9$ photons/s. The ability to detect metal micro- and nanoclusters in silicon using the μ-XRF technique has been well established.[22,23,40] Further details of ALS Beamlines 10.3.1 and 10.3.2 can be found in Ref. 41 and Refs. 42 and 43, respectively. Details of the APS Beamline 2-ID-D zone plate focusing optics[44] and beamline[45] are also available.

In addition to the presence of metal clusters, it is also possible to determine their recombination activity, *in situ* at the synchrotron beamline, using the x-ray beam induced current (XBIC) technique.[46] This technique collects photoexcited minority carriers with a Schottky diode or *p*-*n* junction in a manner similar to laser- or electron-beam induced current (LBIC/EBIC). By simultaneously recording x-ray induced current via a Keithley 428 current amplifier and x-ray fluorescence data via a Princeton Gamma-Tech Prism Si(Li) detector or seven-element Canberra Ge detector for Beamlines 10.3.1 and 10.3.2, respectively, one can concurrently acquire data on the elemental nature and recombination activity of metal clusters in silicon with micron-scale spatial resolution.[47]

To determine the chemical state of Cu in the samples and in the standard materials, μ-XAS was used. μ-XAS is an umbrella group usually divided into two techniques encompassing specific energy ranges: x-ray absorption near-edge microspectroscopy (μ-XANES) spans from the absorption edge onset up to 20–50 eV above the absorption edge onset, and extended x-ray absorption fine-structure microspectroscopy (μ-EXAFS) spans up to several hundred eV above the absorption edge. ALS beamline 10.3.2, which can perform both μ-XANES and μ-EXAFS studies, is equipped with a two-crystal, fixed-exit Si(111) monochromator with an energy resolution of ~ 1 eV. APS Beamline 2-ID-D, which could perform only μ-XANES at the time of this publication, is equipped with a Kohzu Si(111) monochromator with comparable energy resolution.

Because each compound has a unique μ-XAS spectrum—much the same way it has a unique x-ray diffraction (XRD) pattern—a good correlation between μ-XAS spectra from samples and standard material can yield a positive identification of chemical state. Standards consisting of Cu foil, Cu_2O (99+% purity), CuO (97%), and Cu_5Si (99.5%) were acquired from vendors. Standard material of Cu_3Si was prepared at the Institute for Mineralogy at the University of Leipzig. The Cu_3Si reference sample was synthesized by a solid-state reaction from high-purity (>99.999%) silicon and copper in an evacuated silica ampoule at $T = 750\ ^\circ C$. For this purpose, Cu and Si powders were mixed in near-stoichiometric proportions with a slight abundance of Si, dryly homogenized in an agate mortar, and then pressed to a pellet. The sample was annealed as described above for two days and finally quenched in water. The resulting phase was checked by an XRD measurement on a Seifert XRD3000 diffractometer (30 mA/40 kV; Bragg–Brentano geometry) equipped with graphite (002) secondary monochromator and a scintillation detector. The powder-diffraction pattern was recorded from 5° to 110° 2θ, with a step size of 0.01° 2θ and 30 s/step, which confirmed that the resulting material was η-Cu_3Si. The η-Cu_3Si standard material was also measured with XRD *in situ* at ALS Beamline 10.3.2, to confirm the presence of the η-Cu_3Si phase.

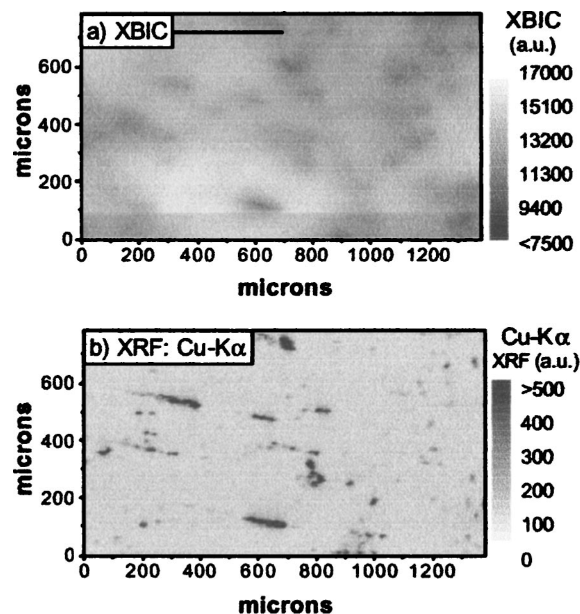

FIG. 1. (a) X-ray beam induced current and (b) Cu $K\alpha$ x-ray fluorescence microscopy maps of float-zone silicon contaminated with $(3-4) \times 10^{16}$ Cu cm^{-3} during crystal growth. Notice the strong correlation between the presence of copper-rich clusters (b) and the decrease of current collection efficiency (a).

μ-XRF, μ-XANES, and μ-EXAFS analyses of samples 1–3 were performed at ALS 10.3.2, in addition to μ-XRF and XBIC analyses of sample 1 at both ALS 10.3.1 and 10.3.2. Additionally, μ-XRF and μ-XANES analyses of sample 4 were performed at APS 2-ID-D. Measurements on standard materials were performed in transmission to avoid overabsorption effects. μ-XAS spectra of Cu-rich clusters in the silicon samples were obtained in fluorescence mode, since the total amount of copper contained in these clusters is below the critical threshold.[42] Standard material was measured at both beamlines ALS 10.3.2 and APS 2-ID-D to ensure that beamline-specific characteristics, such as monochromator energy resolution, would not obscure the direct comparison of spectra obtained at different beamlines.

III. DISTRIBUTION AND CHEMICAL STATE OF Cu-RICH CLUSTERS

Prior to μ-XAS analyses, each Si sample was mapped with μ-XRF to reveal the precise distribution of Cu-rich clusters. The noteworthy observations from μ-XRF maps of each sample are as follows:

(1) For FZ-Si heavily contaminated with Cu during crystal growth (sample 1), irregularly distributed Cu clusters are observed at structural defects [Fig. 1(a)]. This irregular Cu decoration is expected for slow-cooled samples, wherein supersaturated Cu can diffuse to preferred precipitation sites.[48] The observed Cu-rich clusters are strongly recombination active, as revealed by XBIC [Fig. 1(a)]. Five Cu-rich clusters in this sample were analyzed by μ-XAS.

Downloaded 20 Apr 2005 to 131.243.76.24. Redistribution subject to AIP license or copyright, see http://jap.aip.org/jap/copyright.jsp

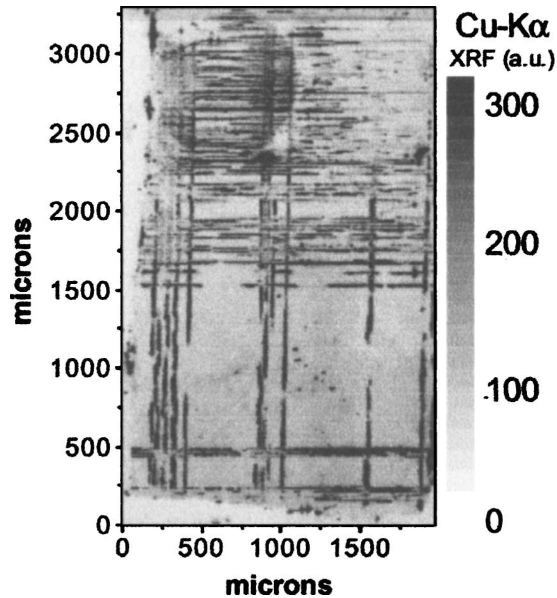

FIG. 2. Cu $K\alpha$ x-ray fluorescence microscopy map of a Cu-contaminated $Si_{0.98}Ge_{0.02}/Si$ heterostructure. The misfit dislocations parallel to the surface, intersecting at 90°, are heavily decorated with clusters of Cu, confirming the tendency of Cu to precipitate in the vicinity of structural defects.

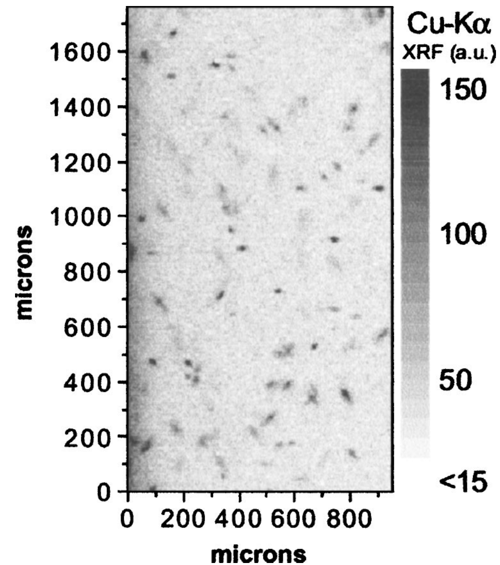

FIG. 3. Cu $K\alpha$ x-ray fluorescence microscopy map of Cu-contaminated Czochralski silicon with $\sim 10^6$ oxygen precipitates per cm^3. Elliptical Cu-rich clusters can be observed, oriented along preferred crystallographic orientations.

(2) Cu-rich precipitates are observed along misfit dislocations in the $Si_{0.98}Ge_{0.02}/Si$ heterostructure (sample 2). From the Cu $K\alpha$ fluorescence map (Fig. 2), one can clearly see the copper contamination along the network of 60° misfit dislocations parallel to the surface, which intersect at 90° angles in agreement with literature observations.[49–51] The recombination activity of these precipitates has been well established by EBIC and XBIC measurements, and is reported elsewhere.[39,49,52] Two Cu-rich clusters were analyzed by μ-XAS in this sample.

(3) In the CZ-Si sample containing 1.8×10^6 cm^{-3} oxygen precipitates (sample 3), $\sim 1.1\times 10^6$ cm^{-3} copper clusters are observed (assuming a Cu $K\alpha$ attenuation length of 70 μm and an angle of 45° between the sample surface normal and the detector). Although each Cu-rich cluster covers many pixels in the μ-XRF map (each pixel=7 $\times 7$ μm^2) to form a disk- or pointlike shape, as evidenced in Fig. 3, the average signal strength within the precipitate is low, evidence for the distribution of Cu in the form of many smaller precipitates. Cu nanoprecipitates have been observed in infrared transmission microscopy,[53] TEM,[33] and etching experiments[13] to form elliptical, platelike, micron-sized colonies of along preferred crystallographic orientations. Interestingly, the elliptical Cu-rich microcolonies observed in μ-XRF also appear to be aligned to certain orientations within the crystal, as shown in Fig. 3. Although the spatial density of these colonies ($\sim 1.1\times 10^6$ cm^{-3}) corresponds well to the density of oxygen precipitates (1.8×10^6 cm^{-3}), the morphology of these Cu clusters appears not to be spherical, indicating that the Cu atoms in this sample preferred not to homogeneously coat the oxygen precipitates, but either used them or their punched out dislocation loops as nucleation sites for Cu microcolony formation. Three Cu-rich clusters were analyzed by μ-XAS in this sample.

(4) In the as-grown cast mc-Si material (sample 4), Cu-rich clusters were located at a grain boundary in the material, together with similar amounts of Ni and less abundant Fe, although no intentional contamination was performed. The μ-XRF map in Fig. 4 shows the Cu distribution along a representative region of the grain boundary. Although the cluster sizes were smaller than the x-ray beam spot size of 200 nm, the number of Cu atoms per cluster was determined to fall within the range of $3\times 10^7 \pm 1.5\times 10^7$ by comparison with standard materials. Were all these Cu atoms contained within one large spherical Cu_3Si particle, following the approximation presented in Ref. 54, the diameters of these particles would range between 100 ± 15 nm. However, it is also possible that these Cu_3Si molecules are distributed among a colony of nanoparticles as reported in TEM studies of intentionally contaminated monocrystalline Si.[33] Seven Cu-rich clusters were analyzed by μ-XANES in this sample.

Cu K-edge μ-XANES scans of the copper-rich clusters in all four samples yielded strikingly similar spectra to Cu_3Si standard material (Fig. 5). A μ-XANES comparison of different standard materials [Fig. 5(a)] reveals that the

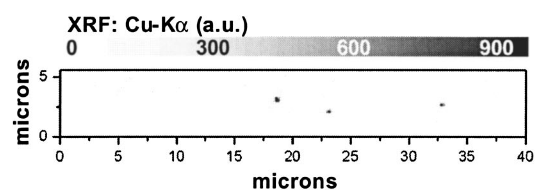

FIG. 4. Cu $K\alpha$ x-ray fluorescence microscopy map along a grain boundary of as-grown cast multicrystalline silicon. Despite no intentional contamination, Cu-rich clusters are present.

Downloaded 20 Apr 2005 to 131.243.76.24. Redistribution subject to AIP license or copyright, see http://jap.aip.org/jap/copyright.jsp

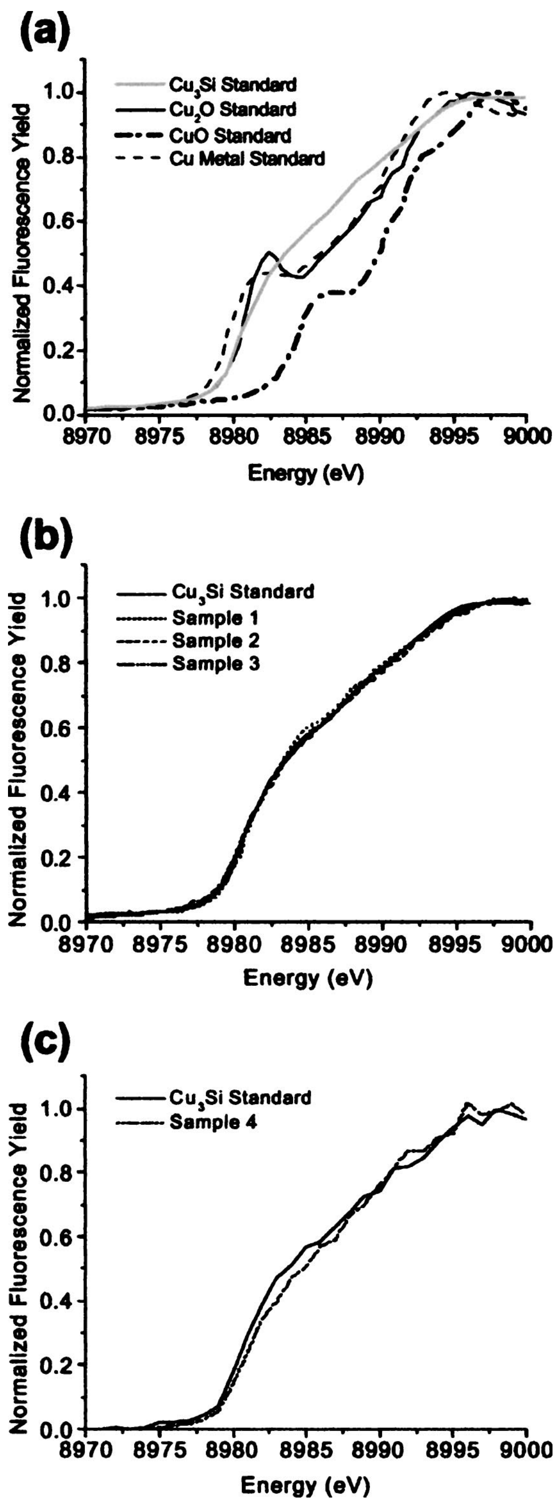

FIG. 5. μ-XANES showing the spectra of standard materials (a), and then the excellent match of Cu-rich clusters in a variety of silicon materials with the Cu_3Si standard (b, c, taken at different beamlines). Sample descriptions are provided in Secs. II and III. Notice in (a) that the edge onset energy of Cu_3Si is not coincident with metallic Cu as would be expected from a metal silicide, but is shifted by +1 eV. This can be understood as an effect of the delocalization of Cu-3d electrons in the presence of Si.

Cu K-edge absorption onset energy of Cu_3Si matches that of the Cu_2O standard, and is shifted as compared to that of metallic Cu standard. The Cu K-edge absorption energy shift of Cu_3Si relative to Cu metal is not typical for all metal silicides. Iron metal and silicides, for example, have identical

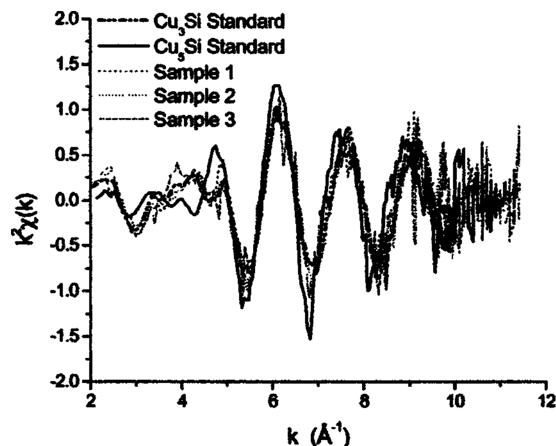

FIG. 6. μ-EXAFS spectra comparing Cu-rich particles in Si with Cu_3Si and Cu_5Si standard materials. It is clear that the chemical form of the Cu-rich clusters within the samples is most similar to the Cu_3Si standard material, not the Cu-rich silicide. Despite variations of copper contamination pathway and oxygen concentration between the three samples, the μ-EXAFS spectra show little deviation from Cu_3Si.

Fe K-edge x-ray absorption onset energies, unlike oxidized iron species that have K-edge onsets shifted to higher energies by amounts proportional to the Fe charge state.[55,56]

In our opinion, this behavior of Cu stems from the unique electronic properties of Cu in Si. Copper dissolved in p-type silicon is well known to diffuse predominantly as Cu_i^+.[1] Recent *ab initio* Hartree–Fock calculations published by Estreicher[5] indicate that Cu_i^+ will not diffuse as a compact $[Ar]3d^{10}4s^0$ sphere, but rather, it will promote some its electrons from the 3d to the 4sp orbitals to form weak covalent bonds with nearby silicon atoms. Similarly, copper atoms precipitated at certain internal voids are predicted to promote a small fraction of their electrons to 4sp orbitals for covalent overlap with neighboring silicon atoms.[5] Macroscopic studies on and models of the properties of copper silicides have also indicated a hybridization of the valence Cu and Si orbitals.[29,57–59] The increased delocalization of Cu valence electrons can qualitatively explain the Cu K absorption edge shift to higher energies; as they are photoexcited out of the atom, Cu 1s core electrons experience a greater Coulombic attraction with the Cu nucleus due to reduced electron screening, and thus require higher x-ray energies for photoionization.

In agreement with the trend observed in the μ-XANES data, the μ-EXAFS spectra of Cu_3Si standard material and Cu-rich clusters in samples 1–3 again match very well, as shown in Fig. 6. It is noticed that the μ-EXAFS data for a more Cu-rich phase of copper silicide, Cu_5Si, are shifted in phase and amplitude relative to the sample data, making a poor fit. It is thus concluded that the chemical form of copper in samples 1–3 is very similar, if not identical, to Cu_3Si, and definitely not an oxidized species nor a copper-rich silicide.

IV. OXIDATION OF COPPER AND OTHER METALS IN Si

In the past, it has been suggested that oxidized metallic precipitates may form within silicon because many species of metal atom, e.g., Cu and Fe, have higher binding energies

Downloaded 20 Apr 2005 to 131.243.76.24. Redistribution subject to AIP license or copyright, see http://jap.aip.org/jap/copyright.jsp

TABLE I. The enthalpies of formation per mol per oxygen atom at 298.15 K for various oxidized metal species. It is shown that the binding energy of oxygen to silicon is far greater than that of oxygen to iron or to copper. The same is not true for all metals, e.g., hafnium. Data are from Ref. 68.

Compound	$\Delta_f H°$ (kJ/mol)
$1/2\ HfO_2$	−572.4
$1/2\ ZrO_2$	−550.3
$1/2\ TiO_2$	−472.0
$1/2\ SiO_2$	−455.4
$1/4\ Fe_2SiO_4$	−370.0
$1/4\ Fe_3O_4$	−279.6
$1/3\ Fe_2O_3$	−274.7
Cu_2O	−168.6
CuO	−157.3

to oxidized compounds such as silicates and oxides than to silicides.[22,27,56] While it is true that metals bond strongly to oxygen, the same can also be said for silicon, and thus an analysis of whether a metallic oxide, silicate, or silicide will form should take this competitive oxidation potential into consideration. It is known that oxygen can form a very stable and electrically inactive interstitial complex with silicon (O_i), not to mention SiO_2. Table I reproduces the enthalpy of formation per oxygen atom (the figure of merit in a balanced equation) from individual elements for a selection of oxidized species, demonstrating that when $[Si] \gg [O] > [Cu]$, equilibrium thermodynamics predicts that silicon will be the predominant oxidized species.

While the precise values of enthalpies of formation cited in Table I do not reflect the additional detailed calculations necessary to account for the formation of a species within a silicon lattice, this treatment provides the conceptual framework from which to analyze the prospect of a metal forming an oxidized species. In the presence of silicon, a strong competitor for oxygen, Cu will likely be reduced or remain unoxidized. This has been demonstrated on a macroscopic level, via the observation that an oxidizing Cu_3Si layer will first form Cu_2O on Cu_3Si, then progress to a final state of SiO_2 on Cu_3Si after annealing.[58] Microscopic calculations predict that although Cu_i is attracted to O_i because it fits nicely into the void at the interstitial site near the O_i, no covalent Cu–O bonding occurs,[60] again confirming that Si wins out over Cu when competing for oxygen. Based on these observations and our μ-XAS measurements, it is concluded that Cu in the presence of Si with $[O] \ll [Si]$ will not tend to form stable chemical bonds with oxygen, and thus will likely either form nonoxidized precipitates, out diffuse, or remain dissolved if solubility permits.

This treatment can be generalized to other metal and metal-oxide or -silicate species. For example, the values in Table I would suggest that Hf would form strong bonds to oxygen even if the heat of formation of hafnium silicide were considered, as was experimentally observed by Murarka and Chang.[61] On the other hand, it appears unlikely that iron will form oxidized precipitates within the silicon bulk, if $[Si] \gg [O] > [Fe]$, as confirmed by multiple sightings of submicron $FeSi_2$ inclusions in mc-Si.[62] A good general review of these thermodynamic principles is presented by d'Heurle *et al.*[63]

There are likely to exist alternative pathways for the introduction of oxidized metal species into mc-Si material. Large oxidized iron particles could be introduced into the melt, survive the crystal growth process, and become trapped, e.g., between grain boundaries during crystal growth. For example, iron in stainless steel readily oxidizes at temperatures above 1000 °C,[55] and the melting temperature of Fe_2O_3 is 150 °C higher than that of silicon. While molten silicon would invariably attack these foreign particles and reduce their size, the observation by McHugo *et al.*[56] of partially oxidized Fe inside a Fe+Ni+Cr particle cluster >15 μm in diameter seems to suggest that this contamination pathway may indeed occur. The same pathway is not predicted to occur for oxidized Cu particles, as the low melting temperatures of both Cu_2O (1235 °C) and CuO (1326 °C) imply that such particles would quickly dissolve in molten silicon (1414 °C). Experimental evidence up to this point has shown no evidence for oxidized Cu-rich clusters inside silicon crystals.

V. Al GETTERING AND DISSOLUTION OF Cu PRECIPITATES

Aluminum gettering was performed on a Cu-contaminated sample to study the gettering mechanism and its effectiveness. A 700-μm-thick CZ sample containing $10^6\ cm^{-3}$ oxygen precipitates was copper contaminated by a diffusion anneal at 1200 °C. After the sample was cooled to room temperature, a 5-μm aluminum layer was evaporated onto one surface of the sample through a wire mesh. Subsequently, the sample was annealed at 800 °C for 2 h in forming gas ambient in a horizontal furnace to getter the Cu to the Al. The sample was then removed from the furnace onto an aluminum plate, where it cooled rapidly.

The aluminum gettering layer was subsequently observed with an optical microscope [Fig. 7(a)] and scanned with μ-XRF [Fig. 7(b)], revealing copper present only where aluminum was deposited through the wire mesh. No Cu was detected in an Al layer of the same thickness evaporated onto a float-zone control sample, which confirms cleanliness of the evaporated aluminum. The effectiveness of aluminum gettering for the removal of Cu from bulk Si is a likely indication of a weak binding energy of Cu to Cu_3Si clusters, unlike what one would expect from an oxidized species.

The chemical state of Cu in the Al gettering layer provides an indication of the gettering mechanism. μ-EXAFS analyses of the chemical state of copper gettered to thicker regions of Al [indicated by a dashed arrow in Fig. 7(b)] indicate that copper has formed a species very similar to that identified in Ref. 64, a dilute Cu solution in Al (Fig. 8). This result directly confirms the generally accepted opinion[65] that the mechanism of segregation of metals in aluminum is their higher solubility in the liquid phase.

A different chemical state of Cu is identified in thinly dispersed aluminum particles on the backside [indicated by a solid arrow in Fig. 7(b)]. The μ-EXAFS from this location

Downloaded 20 Apr 2005 to 131.243.76.24. Redistribution subject to AIP license or copyright, see http://jap.aip.org/jap/copyright.jsp

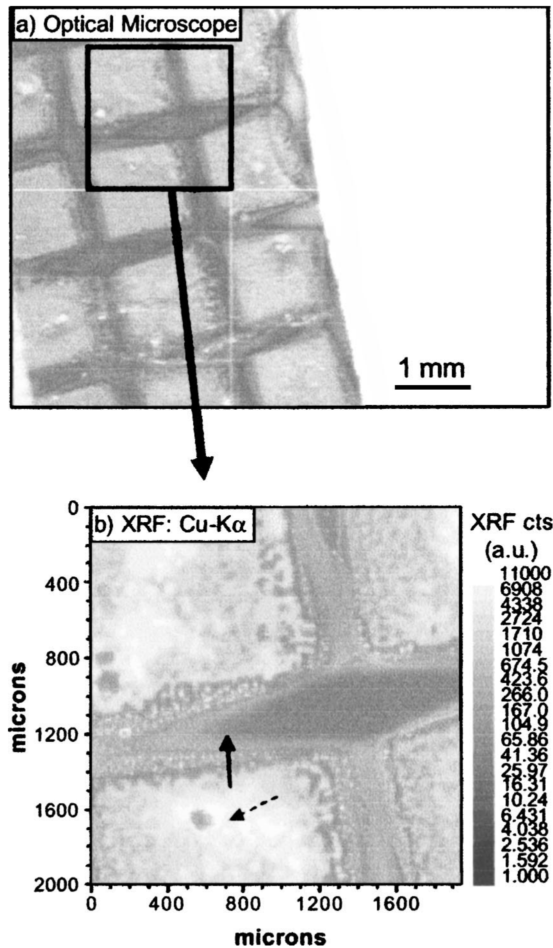

FIG. 7. (a) Optical microscope image of the surface of a Cu-contaminated CZ-Si sample with 10^6 cm^{-3} oxygen precipitates. This sample was annealed at 800 °C for 2 h after squares of aluminum were evaporated onto the surface through a wire mesh. (b) Cu $K\alpha$ x-ray fluorescence microscopy image for the region highlighted in (a) shows the high concentration of Cu gettered to the thick Al squares (note log XRF scale), and the fine dusting of Cu in tiny Al particles between the squares. The dashed and solid arrows denote locations of μ-EXAFS scans in Figs. 7 and 8, respectively.

(Fig. 9), while not making a perfect match with any of our standards, is most similar to the θ-Al_2Cu standard material of Ref. 64. Precipitates of θ-Al_2Cu, which are known to form within aluminum layers, are very unstable and dissolve rapidly at temperatures above 400 °C. Therefore, there is no indication that the presence of this phase would change the segregation coefficient of copper to aluminum at higher temperatures. At the moment, it cannot be unambiguously determined why this different phase of copper is observed only in thin Al layers. One may speculate that the percentage composition of copper in the thin aluminum layer increased substantially during cooldown, either via relaxation gettering of copper from the bulk and/or a strong temperature dependence of the segregation coefficient. It has been observed, for example, that Al is effective at gettering Cu from Si at temperatures as low as 540 °C.[34]

The increased solubility of Cu in the Al gettering layer, the presumably weak binding energy of Cu to Cu_3Si, and the high diffusivity of Cu in Si suggest that Al gettering is indeed very effective for removing Cu from bulk silicon. However, this does not imply that a standard Al gettering procedure, with a micron of Al and an 800 °C anneal, would remove all Cu from the Si bulk to below the detection limit. The residual concentration of Cu in the silicon wafer after Al gettering is determined by three parameters, the thicknesses of the silicon substrate, the thickness of the aluminum layer, and the segregation coefficient, i.e., the ratio of the equilibrium solubilities of copper in aluminum (c_{Al}) and in silicon (c_{bulk}) at a given temperature

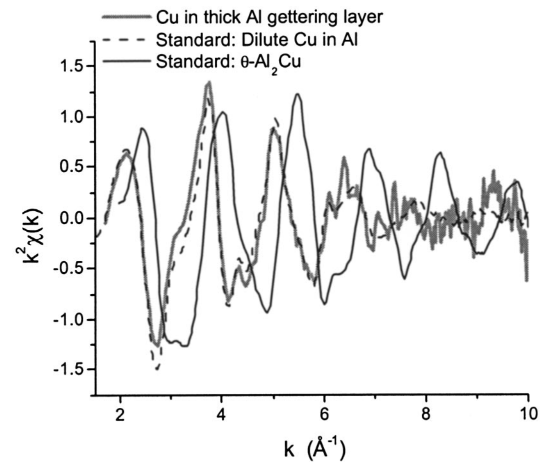

FIG. 8. EXAFS of Cu gettered to thick regions of Al [dashed arrow in Fig. 6(b)]. Notice the fairly good agreement with the standard material of dilute Cu dissolved in Al. (Standards from Ref. 64.)

$$k_T \equiv \frac{c_{\mathrm{Al}}}{c_{\mathrm{bulk}}}. \tag{1}$$

The segregation coefficient k can be derived experimentally from the μ-XRF map in Fig. 7(b) by taking into consideration the Cu counts in the thick Al layer versus the counts in the bare silicon bulk, the thicknesses of these two layers, and the XRF attenuation lengths of the Cu $K\alpha$ fluorescence signal in these two layers. The segregation coefficient as defined in Eq. (1) for the sample shown in Fig. 7(b) is estimated to be *at least* $(1-2)\times 10^3$. This value is a lower

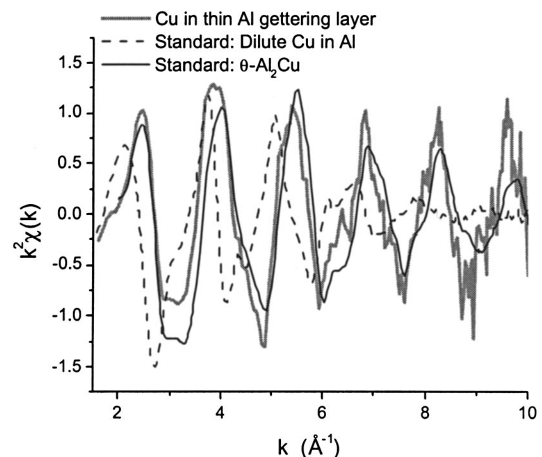

FIG. 9. EXAFS of Cu gettered to thin regions of Al [solid arrow in Fig. 6(b)]. Notice the difference between this spectrum and that of the thicker regions of Al (Fig. 7). The progression of the measured spectrum from dilute Cu in Al to q-Al_2Cu indicates an increasing saturation of Al with gettered Cu. (Standards are from Ref. 64.)

Downloaded 20 Apr 2005 to 131.243.76.24. Redistribution subject to AIP license or copyright, see http://jap.aip.org/jap/copyright.jsp

estimate since a parasitic background Cu signal measured by the fluorescence detector, although much too weak to disturb μ-XAS measurements, is likely to have produced an artificially high Cu count rate on the bare silicon bulk. Nevertheless, this value is close to what one would expect assuming a solubility of Cu in the Al–Si layer of about 0.1–1 at. % and a Cu solubility in Si at 800 °C of 5.5×10^{16} cm^{-3}, while being consistent with earlier results[35] providing $k>1\times10^3$.

With the estimated segregation coefficient $k=2\times10^3$ and typical solar cell parameters for wafer thickness $d=240$ μm and Al layer thickness $w=1$ μm, one can predict from the following equation (from Ref. 66):

$$\frac{[\mathrm{Cu}]\text{ in bulk after gettering}}{[\mathrm{Cu}]\text{ in bulk before gettering}} \equiv \frac{c_{\mathrm{bulk}}}{c_0} = \frac{c_{\mathrm{bulk}}}{\left[\dfrac{(c_{\mathrm{bulk}}\times d)+(c_{\mathrm{Al}}\times w)}{d}\right]} = \frac{1}{1+\dfrac{k\times w}{d}} \tag{2}$$

that an upper limit of about 90% of the total copper content can be gettered from the bulk by segregation to the Al layer. With a ten times higher segregation coefficient, $k=10^4$, and all other parameters constant, the same calculation predicts an upper limit of over 97%.

It follows from Eq. (2) that the much lower thickness of the Al layer than that of the Si wafer leads to a much faster increase of Cu concentration in the Al layer than its decrease in Si. Thus, when equilibrium is reached, Cu concentration in the bulk may only decrease by a relatively small factor. It is likely that the remaining dissolved Cu in the bulk will reprecipitate during cooling, especially with the high density of structural defects present in mc-Si. This is consistent with numerous μ-XRF observations of Cu-rich clusters at structural defects in Al-gettered or fully processed mc-Si.[21,23–25] Irrespective of the precise value of k, it follows from Eq. (2) that thicker Al layers should result in the removal of a larger fraction of the total Cu from the bulk during gettering.

Other mechanisms may also be responsible for retarding or inhibiting the complete dissolution and removal of all Cu_3Si clusters during gettering. Cu_3Si clusters, or individual Cu atoms, may be stabilized either by the lattice strains of adjacent structural defects or other metal clusters.[21,67] Specifically, the chemical interactions between Cu and other metal species (of which mc-Si contains an abundance[24,26]) are not well understood at the present time. The singular result of all these effects would likely be a somewhat lower effective segregation coefficient for mc-Si than that for single-crystalline silicon (sc-Si). As a consequence, more Cu is likely to remain within bulk mc-Si after Al gettering than sc-Si. Additionally, it has also been suggested that relatively slowly diffusing Si self-interstitials may play a rate-limiting role in precipitate dissolution, as these are needed to counterbalance the volumetric shrinkage associated with the dissolving Cu_3Si precipitates.[27] In any case, a two-step aluminum gettering treatment, consisting of a high-temperature step to fully dissolve Cu from Cu_3Si clusters, followed by a gradual lowering of the temperature to promote the diffusion of Cu_i^+ to the Al gettering layer, may be a viable alternative to optimize the removal of Cu from bulk Si.

VI. SUMMARY AND CONCLUSIONS

Synchrotron-based x-ray microprobe techniques have been employed to identify the chemical state of copper clusters in a variety of silicon materials with varying degrees of copper contamination and oxygen concentrations. A good match of μ-XAS spectra between Cu-rich clusters in Si and Cu_3Si standard material allows one to conclude that Cu-rich clusters in all four studied materials are indeed Cu_3Si. In the μ-XANES analyses, the K absorption edge of Cu_3Si is shifted to higher energies. This can be explained by the delocalization of some Cu-3d valence electrons in the presence of silicon neighbors due to the covalent character of the bonding. The absorption onset edge shift is concluded not to be due to the oxidation of Cu atoms within these clusters.

The likelihood of forming oxidized metal species within silicon is discussed on the basis of this experimental evidence, previous work, and thermodynamic considerations. It is concluded that certain metals such as Cu and Fe are unlikely to form oxidized species within a silicon matrix because silicon bonds to oxygen more strongly than do these metals. On the other hand, certain metals such as Hf bond to O more strongly than does Si, and thus it is predicted that those metals will form oxidized complexes in Si. Furthermore, the possibility is suggested that oxidized iron particles may be present in mc-Si wafers via contamination of the melt by foreign particles.

Aluminum gettering is shown to be very effective at gettering copper from silicon, a natural consequence of the fact that copper is only weakly bound to copper silicide particles, and thus at higher temperatures Cu can readily diffuse to the Al layer where its solubility was experimentally determined to increase by at least three orders of magnitude. μ-EXAFS reveals that the chemical state of Cu in thick Al gettering layers matches well that of a solid solution of Cu in Al, consistent with the notion that the mechanism of segregation of copper in aluminum is its higher solubility in the liquid phase, which does not necessarily imply any chemical bonding of copper to aluminum. Despite its effectiveness, Al gettering does not remove all Cu from the bulk. The segregation coefficient and the relative thicknesses of the Al and Si layers determine the ungettered fraction of Cu, which may promptly reprecipitate at the most stable heterogeneous nucleation sites within the bulk upon cooling. In addition, a few possible mechanisms retarding the dissolution of Cu_3Si clusters have been described, namely, stabilization by the lattice strains of nearby structural defects and/or other metal clusters.

ACKNOWLEDGMENTS

Many thanks go to S. K. Estreicher and M. A. Van Hove for the useful discussions concerning the delocalization of Cu valence electrons in Si, to J. Kalejs and R. Gronsky for suggestions concerning metal inclusion formation during crystal growth, to U. Wulf for discussion of thermodynamics, and to W. Schröter for encouraging discussion. We are much obliged to W. Seifert and M. Kittler for providing the SiGe/Si heterostructure. This work was funded by NREL Subcontract No. AAT-2-31605-03. One of the authors

Downloaded 20 Apr 2005 to 131.243.76.24. Redistribution subject to AIP license or copyright, see http://jap.aip.org/jap/copyright.jsp

(M.H.) thanks the Deutsche Forschungsgemeinschaft for funding the project HE 3570/1-1. Impurity-doped float-zone silicon crystal growth at the National Renewable Energy Laboratory was supported by U.S. Department of Energy Contract No. DE-AC36-99G010337. The operations of the Advanced Light Source at Lawrence Berkeley National Laboratory are supported by the Director, Office of Science, Office of Basic Energy Sciences, Materials Sciences Division, of the U.S. Department of Energy under Contract No. DE-AC03-76SF00098. Use of the Advanced Photon Source was supported by the U.S. Department of Energy, Office of Science, Office of Basic Energy Sciences, under Contract No. W-31-109-ENG-38.

[1] R. N. Hall and J. H. Racette, J. Appl. Phys. **35**, 379 (1964).
[2] E. R. Weber, Appl. Phys. A: Solids Surf. **30**, 1 (1983).
[3] A. A. Istratov, C. Flink, H. Hieslmair, E. R. Weber, and T. Heiser, Phys. Rev. Lett. **81**, 1243 (1998).
[4] A. A. Istratov and E. R. Weber, J. Electrochem. Soc. **149**, G21 (2002).
[5] S. K. Estreicher, Phys. Rev. B **60**, 5375 (1999).
[6] J.-L. Maurice and C. Colliex, Appl. Phys. Lett. **55**, 241 (1989).
[7] A. Broniatowski, Philos. Mag. B **66**, 767 (1992).
[8] A. A. Istratov *et al.*, J. Electrochem. Soc. **145**, 3889 (1998).
[9] M. Seibt, H. Hedemann, A. A. Istratov, F. Riedel, A. Sattler, and W. Schröter, Phys. Status Solidi A **171**, 301 (1999).
[10] R. Sachdeva, A. A. Istratov, and E. R. Weber, Appl. Phys. Lett. **79**, 2937 (2001).
[11] M. Seibt, in *Crystalline Defects and Contamination: Their Impact and Control in Device Manufacturing II*, edited by B. O. Kolbesen, C. Claeys, P. Stallhofer, and F. Tardif (The Electrochem. Soc., Pennington, 1997), p. 243.
[12] M. Seibt, in *Semiconductor Silicon 1990*, edited by H. R. Huff, K. G. Barraclough, and J. I. Chikawa (The Electrochem. Soc., Pennington, 1990), p. 663.
[13] M. Seibt and K. Graff, J. Appl. Phys. **63**, 4444 (1988).
[14] C. Flink, H. Feick, S. A. McHugo, W. Seifert, H. Hieslmair, T. Heiser, A. A. Istratov, and E. R. Weber, Phys. Rev. Lett. **85**, 4900 (2000).
[15] W. C. Dash, J. Appl. Phys. **27**, 1193 (1956).
[16] B. Shen, T. Sekiguchi, J. Jablonski, and K. Sumino, J. Appl. Phys. **76**, 4540 (1994).
[17] W. C. Dash, J. Appl. Phys. **30**, 459 (1959).
[18] A. J. R. de Kock, Appl. Phys. Lett. **16**, 100 (1970).
[19] J. P. Kalejs, B. Bathey, and C. Dubé, J. Cryst. Growth **109**, 174 (1991).
[20] Report IEA-PVPS T1–12:2003, International Energy Agency—Photovoltaic Power Systems Programme, 2003 (in press).
[21] S. A. McHugo, Appl. Phys. Lett. **71**, 1984 (1997).
[22] S. A. McHugo *et al.*, J. Appl. Phys. **89**, 4282 (2001).
[23] A. A. Istratov, H. Hieslmair, O. F. Vyvenko, E. R. Weber, and R. Schindler, Sol. Energy Mater. Sol. Cells **72**, 441 (2002).
[24] A. A. Istratov, T. Buonassisi, R. J. McDonald, A. R. Smith, R. Schindler, J. A. Rand, J. P. Kalejs, and E. R. Weber, J. Appl. Phys. **94**, 6552 (2003).
[25] T. Buonassisi *et al.*, J. Appl. Phys. **95**, 1556 (2004).
[26] D. Macdonald, A. Cuevas, A. Kinomura, and Y. Nakano, in *29th Photovoltaic Specialists Conference Proceedings* (IEEE, New Orleans, USA, 2002), p. 285.
[27] S. A. McHugo, A. Mohammed, A. C. Thompson, B. Lai, and Z. Cai, J. Appl. Phys. **91**, 6396 (2002).
[28] E. Nes and J. Washburn, J. Appl. Phys. **43**, 2005 (1972).
[29] G. Das, J. Appl. Phys. **44**, 4459 (1973).
[30] E. Nes and G. Lunde, J. Appl. Phys. **43**, 1835 (1972).
[31] J. K. Solberg, Acta Crystallogr., Sect. A: Cryst. Phys., Diffr., Theor. Gen. Crystallogr. **34**, 684 (1978).
[32] R. Rizk, X. Portier, G. Allais, and G. Nouet, J. Appl. Phys. **76**, 952 (1994).
[33] M. Seibt, M. Griess, A. A. Istratov, H. Hedemann, A. Sattler, and W. Schröter, Phys. Status Solidi A **166**, 171 (1998).
[34] R. D. Thompson and K. N. Tu, Appl. Phys. Lett. **41**, 440 (1982).
[35] L. A. Verhoef, P. P. Michiels, S. Roorda, W. C. Sinke, and R. J. C. Van Zolingen, Mater. Sci. Eng., B **7**, 49 (1990).
[36] H. Hieslmair, S. A. McHugo, and E. R. Weber, in *25th IEEE Photovoltaic Specialists Conference* (IEEE, Washington D.C., 1996), p. 441.
[37] G. A. Petersen and S. M. Myers, J. Appl. Phys. **89**, 4269 (2001).
[38] T. F. Ciszek and T. H. Wang, J. Cryst. Growth **237–239**, 1685 (2002).
[39] M. Kittler, C. Ulhaq-Bouillet, and V. Higgs, J. Appl. Phys. **78**, 4573 (1995).
[40] T. Buonassisi *et al.*, Physica B **340–342**, 1137 (2003).
[41] J. H. Underwood, A. C. Thompson, Y. Wu, R. D. Giauque, K. W. Jones, and M. L. Rivers, Nucl. Instrum. Methods Phys. Res. A **266**, 318 (1988).
[42] A. Manceau, M. A. Marcus, and N. Tamura, in *Applications of Synchrotron Radiation in Low-temperature Geochemistry and Environmental Science*, edited by P. Fenter and N. C. Sturchio (Mineralogical Society of America, Washington D.C., 2002), Vol. 49, p. 341.
[43] M. A. Marcus, A. A. MacDowell, R. Celestre, A. Manceau, T. Miller, H. A. Padmore, and R. E. Sublett, J. Synchrotron Radiat. **11**, 239 (2004).
[44] W. Yun *et al.*, Rev. Sci. Instrum. **70**, 2238 (1999).
[45] Z. Cai, B. Lai, W. Yun, P. Ilinski, D. Legnini, J. Maser, and W. Rodrigues, AIP Conf. Proc. **521**, 31 (2000).
[46] O. F. Vyvenko, T. Buonassisi, A. A. Istratov, H. Hieslmair, A. C. Thompson, R. Schindler, and E. R. Weber, J. Appl. Phys. **91**, 3614 (2002).
[47] O. F. Vyvenko, T. Buonassisi, A. A. Istratov, and E. R. Weber, J. Phys.: Condens. Matter **16**, S141 (2003).
[48] B. Shen, T. Sekiguchi, R. Zhang, Y. Shi, H. Shi, K. Yang, Y. Zheng, and K. Sumino, Jpn. J. Appl. Phys., Part 1 **35**, 3301 (1996).
[49] T. S. Fell and P. R. Wilshaw, J. Phys. IV **1**, C6 (1991).
[50] D. M. Lee and G. A. Rozgonyi, Appl. Phys. Lett. **65**, 350 (1994).
[51] G. Kissinger, G. Morgenstern, and H. Richter, J. Appl. Phys. **75**, 4994 (1994).
[52] O. F. Vyvenko, T. Buonassisi, A. A. Istratov, E. R. Weber, M. Kittler, and W. Seifert, J. Phys.: Condens. Matter **14**, 13079 (2002).
[53] G. H. Schwuttke, J. Electrochem. Soc. **108**, 163 (1961).
[54] S. A. McHugo *et al.*, J. Cryst. Growth **210**, 395 (2000).
[55] N. T. Barrett, P. N. Gibson, G. N. Greaves, P. Mackle, K. J. Roberts, and M. Sacchi, J. Phys. D **22**, 542 (1989).
[56] S. A. McHugo, A. C. Thompson, G. Lamble, C. Flink, and E. R. Weber, Physica B **273–274**, 371 (1999).
[57] L. Magaud, S. Guillet, and T. Lopez-Rios, Physica B **225**, 225 (1996).
[58] A. Cros, M. O. Aboelfotoh, and K. N. Tu, J. Appl. Phys. **67**, 3328 (1990).
[59] Z. An, C. Kamezawa, M. Hirai, M. Kusaka, and M. Iwami, J. Phys. Soc. Jpn. **71**, 2948 (2002).
[60] D. West, S. K. Estreicher, S. Knack, and J. Weber, Phys. Rev. B **68**, 035210 (2003).
[61] S. P. Murarka and C. C. Chang, Appl. Phys. Lett. **37**, 639 (1980).
[62] T. Buonassisi *et al.*, in *13th Workshop on Crystalline Silicon Solar Cell Materials and Processes*, edited by B. Sopori (NREL, Golden, CO, 2003), p. 96.
[63] F. M. d'Heurle, A. Cros, R. D. Frampton, and E. A. Irene, Philos. Mag. B **55**, 291 (1987).
[64] M. A. Marcus and J. E. Bower, J. Appl. Phys. **82**, 3821 (1997).
[65] M. Apel, I. Hanke, R. Schindler, and W. Schröter, J. Appl. Phys. **76**, 4432 (1994).
[66] H. Hieslmair, S. A. McHugo, A. A. Istratov, and E. R. Weber, in *Properties of Crystalline Silicon*, edited by R. Hull (INSPEC, Exeter, 1999), p. 775.
[67] M. Kittler and W. Seifert, Solid State Phenom. **95–96**, 197 (2004).
[68] *CRC Handbook of Chemistry and Physics*, edited by David R. Lide (CRC, Boca Raton, 2003), 84th ed.

Downloaded 20 Apr 2005 to 131.243.76.24. Redistribution subject to AIP license or copyright, see http://jap.aip.org/jap/copyright.jsp